

High grade glioma diffusive modeling using statistical tissue information and diffusion tensors extracted from atlases

A. Roniotis, G. Manikis, V. Sakkalis, M. Zervakis, *Member, IEEE*, I. Karatzanis, and K. Marias, *Member, IEEE*

Abstract -Glioma, especially glioblastoma, is a leading cause of brain cancer fatality involving highly invasive and neoplastic growth. Diffusive models of glioma growth use variations of the diffusion – reaction equation in order to simulate the invasive patterns of glioma cells by approximating the spatiotemporal change of glioma cell concentration. The most advanced diffusive models take into consideration the heterogeneous velocity of glioma in gray and white matter, by using two different discrete diffusion coefficients in these areas. Moreover, by using Diffusion Tensor Imaging (DTI), they simulate the anisotropic migration of glioma cells, which is facilitated along white fibers, assuming diffusion tensors with different diffusion coefficients along each candidate direction of growth. Our work extends this concept by fully exploiting the proportions of white and gray matter extracted by normal brain atlases, rather than discretizing diffusion coefficients. Moreover, the proportions of white and gray matter, as well as the diffusion tensors, are extracted by the respective atlases, thus no DTI processing is needed. Lastly, we applied this novel glioma growth model on real data and the results indicate that prognostication rates can be improved.

glioma, diffusive modeling, brain atlas, tissue proportion, anisotropic growth

I. INTRODUCTION

Cancer is a leading cause of death worldwide (causing around 13% of all deaths), with deaths being projected to continue rising, with an estimated 12 millions in 2030 [1, 2]. Out of these, 2.5% of cancer deaths in United States are caused by brain tumors [3], with glioma accounting for 44.4% of them. More specifically, glioblastoma multiforme (GBM) is the most common glioma tumor, accounting 52% of glioma cases and 20% of intracranial brain tumors [4-6].

Glioblastoma is a grade IV astrocytoma, having the worst prognosis of any other malignancy of the Central Nervous System, with survival time ranging from 6 of 14 months after diagnosis and less than 4% of treated patients being alive after 5 years [7-11]. GBM is the most malignant form of brain tumor,

mainly characterized by aggressive and rapid infiltration against neighboring normal tissue [12-13]. Unfortunately, the detection rates of the exact tumor boundaries with common imaging techniques such as magnetic resonance imaging (MRI), X-ray computed tomography (CT) and positron emission tomography (PET) are still poor [14], mainly because these tumors do not form a solid and compact mass.

Since early 90s, there has been a vast amount of research towards simulating and mathematically formulating the mechanisms that govern the development of glioma, both in macroscopic and microscopic levels. Proper treatment planning requires knowing both where the tumor mass is located and whether the occult cancer cells have infiltrated in nearby healthy tissue. To this end, glioma computational models have been studied, towards facilitating the prediction of tumor expansion. Microscopic models [15-19] study the intracellular interactions and biological dependencies in cell level, while macroscopic approximations study the tumor behavior, velocity and mass deformation with using anatomical information derived from medical images [20-26].

Special attention has been given to a specific class of macroscopic models, namely diffusive models [27]. The latter make use of diffusion – reaction approaches in order to couple the invasive migration of glioma cells (diffusion) with the mechanism of proliferation (reaction). They all use variations of the diffusion reaction equation (DRE) to simulate the spatiotemporal change of tumor cell density.

II. BACKGROUND

A. Diffusive Modeling

Mathematical modeling of glioma at the macroscopic level has represented the traditional framework in predicting glioma diffusion. Kansal et al. [28] viewed the tumor as a Gompertzian population of cells and its growth as a dynamic process where proliferating and inactive classes of cells interact, without taking invasion into neighboring tissues into account. Moreover, Zizzari's volumetric model [29] describes the proliferation of GBMs using tensor product splines and differential equations, the solutions of which give the spatiotemporal distribution of tumor cells. Finally, Tabatabai et al. [30] simulate tumor asymmetric growth by accommodating the concept of increasing versus decreasing tumor radii, without incorporating the interactions between healthy and cancer cells at the tumor border and the competition of cells

Manuscript received April 12, 2011. Present work was partially supported by the community initiative program INTERREG III, project "YIIEP@EN", financed by the EC through the European Regional Development Fund (ERDF) and by national funds of Greece and Cyprus. This work was also supported in part by the EC under the project TUMOR (FP7-ICT-2009.5.4-247754).

A. Roniotis, G. Manikis, V. Sakkalis, I. Karatzanis and K. Marias are with the Institute of Computer Science, Foundation for Research and Technology, Greece (e-mail: {roniotis; gmanikis; sakkalis; karatzan; kmarias}@ics.forth.gr)

A. Roniotis and M. Zervakis (michalis@display.tuc.gr) are with the Dept. of Electronic & Computer Engineering, Technical University of Crete, Greece..

inside the tumor. However, even if these macroscopic models used growth and proliferation parameters, they don't produce realistic clinical cancer growth representation.

On the other hand, the trend in glioma research is to study biological and clinical factors involved in cancer diffusion through healthy tissue. Diffusive models were introduced to address this direction. Diffusive models simulate the change of glioma cell concentration in time and in space, by using two main terms of the DRE. The first term expresses the diffusive behavior of tumor cells and the way they are dispersed in brain, while the second one constitutes the net proliferation rate of glioma cells. In 1995, Tracqui et al. [20] introduced the formalism of the DRE as:

$$\frac{\partial c(\mathbf{x}, t)}{\partial t} = \text{div}(D\nabla c(\mathbf{x}, t)) + f(c(\mathbf{x}, t)) \quad (1)$$

where $c(\mathbf{x}, t)$ is the tumor concentration in position $\mathbf{x} = (x, y, z)$ at time t , D is the diffusion coefficient, ∇ and div are the gradient and divergence operators respectively, and $f(c)$ is the net cell proliferation rate. In that model, the tumor cells are assumed to diffuse isotropically and the simulations were run in 2-D slices, extracted from CT scans.

In 2000 Swanson et al. [21] took also into account biological phenomena underlying the migration of glioma, such as the high velocity of glioblastoma in myelinating sheaths. Simulations of this proliferation – diffusion equation were performed on a 3D MR structural image of the brain, with segmentation of white and gray matter (WM, GM). Thus, equation (1) was changed to:

$$\frac{\partial c(\mathbf{x}, t)}{\partial t} = \text{div}(D(\mathbf{x})\nabla c(\mathbf{x}, t)) + f(c(\mathbf{x}, t)) \quad (2)$$

where $D(\mathbf{x})$ is the local diffusion coefficient, taking two discrete values: D_g and D_w for \mathbf{x} being in GM and WM respectively. In that model, D_w is assumed to be five times larger than D_g for high grade glioma, according to the clinical observations of Giese et al. [31, 32], where diffusion speed was found to be faster in WM as compared to GM.

In 2004, Price et al. opened the way for simulating the anisotropic growth of tumor along white matter fibers [6], in conjunction with the tracked fiber pathways [33]. Price et al. used T2- and Diffusion Tensor Imaging (DTI) MRIs scans to determine whether DTI can identify abnormalities that appeared normal on T2. In order to incorporate the experimental findings supporting that the migration of glioma cells is facilitated along white fibers, in 2005, Jbabdi et al. and Clatz et al. [22, 24] extended the model of equation (2) by introducing the local diffusion tensors derived from water diffusion, instead of gradient diffusion coefficients. Both models are based on MRIs and DTI-MRIs and take into account local geometry and directionality of white matter tracks, using the following advanced version of equation (2):

$$\frac{\partial c(\mathbf{x}, t)}{\partial t} = \text{div}(\mathbf{D}(\mathbf{x})\nabla c(\mathbf{x}, t)) + f(c(\mathbf{x}, t)) \quad (3)$$

where $\mathbf{D}(\mathbf{x})$ is the local diffusion tensor which describes the directional tumor cell diffusion, i.e. a 3-by-3 symmetric positive definite matrix. Moreover, Clatz et al. used biomechanics to simulate the deformation of the surrounding area, due to tumor growth and pressure. In 2007, Hogeia et al. [26] extended the anisotropic model by introducing an advection term in (2), with a two-way coupling with the underlying tissue elastic deformation. Later, Morris et al. [34]

used supervised learning algorithms to learn this general model, by observing the growth patterns of glioma from other patients. Continuing, Konukoglu et al. [25] adapted the model to the specific patient cases, using successive sessions of MRIs. Eikonal Equations were used to couple the reaction - diffusion dynamics with tumor evolution.

B. Therapy Modeling

Models that incorporate therapy parameters could be used for optimizing therapy results, because radiologists could predict the response of the patients to different therapeutic schemes. Several approaches have been published towards simulating radiotherapy and chemotherapy, by adjusting the proliferation term $f(c)$, which refers to the net cell birth rate. The net cell proliferation rate $f(c)$ actually consists of the net birth term ($B(c)$) minus the treatment term ($T(c)$). Some functions that have been proposed [35] for the net birth rate $B(c)$ follow the geometric law:

$$B(c) = \rho c, \quad (4a)$$

the Verhulst law (logistic law):

$$B(c) = \rho c \frac{c_m - c}{c_m} \quad (4b)$$

and the Gompertzian law:

$$B(c) = \rho c \ln \frac{c_m}{c}, \quad (4c)$$

where ρ is the geometrical growth parameter and c_m is the maximum tumor cell concentration parameter. For most cases, (4a) and (4b) are used. Under these conditions, in order to simulate radiotherapy and chemotherapy, someone should adjust the treatment term $T(t)$ to incorporate the therapeutic scheme. Swanson et al. [36] predicted survival time after resection by estimating two biological factors, the net rates of proliferation and diffusion, and their ratio from pre-treatment gadolinium-enhanced T1-weighted and T2-weighted MR images. Rockne et al. [37] simulated radiotherapy by introducing the radiobiology parameters α and β into $T(t)$, which are interpreted biologically as repairable single and lethal double-strand breaks to the cell's DNA, respectively [38]. Lastly, some important works have been proposed for non diffusive models of glioma, taking into account the biological mechanisms involved in tumor and normal tissue [39-40].

This paper fully exploits a new approach for extending the anisotropic and heterogeneous diffusion - reaction equation, which has been recently proposed in Sakkalis et al. [41] where only some preliminary results were presented. Instead of using two discrete values for diffusion coefficients in WM and GM, the model uses continuous values, indicating the proportion of white and gray matter in each voxel. Moreover, it has been observed in some cases that a portion of cancer cells can spread in the cerebrospinal fluid (CSF), causing symptoms similar to meningitis - headaches, sickness, and problems with sight and movement [42, 43]. For large glioma, in which proliferating cells may leak to CSF, this could be simulated by setting a non-zero diffusion coefficient for CSF voxels. The proportion of GM, WM and CSF in each voxel of the patient data has been extracted from the SRI24 atlas [44, 45], which is an MRI-based atlas of normal adult human brain anatomy, generated by registering images of 24 normal brains. In order to apply the model the patient MRI data is initially registered and interpolated to the normal atlas slices. Then, glioblastoma is annotated and delineated on the interpolated patient data by an

expert radiologist, before simulating the growth of tumor using the new proposed method. Our hypothesis is that the proposed proportional model proposed can, in most cases, predict glioma growth more effectively than the two standard diffusive models: uniform radial growth across all tissue types and faster diffusion in white matter. An overview of the modeling flow is presented in Fig. 1, which depicts the simulation procedure.

This paper presents a new diffusive model with an extended DRE framework of weighting tensors. By using these tensors, the model fully exploits the spatial proportion of gray and white matter provided by brain atlases, rather than using discrete diffusion coefficients. Moreover, DTI data required for simulating anisotropic growth along white fibers can be replaced by tensors extracted by atlases. The paper proceeds as follows: Section II presents background information on the problem peculiarities and the solution approaches. Section III describes the architecture of the model and the simulation flow. Section IV demonstrates some simulations on real clinical datasets. The last two sections conclude the analysis with general discussion and review of the paper contributions.

III. METHODS

A. Tissue heterogeneity and anisotropic diffusion model

Our biologically based modeling efforts are based on the hypothesis that glioma can be characterized by two net rates, namely proliferation and invasion, which are included in the diffusion - reaction equation (3). Diffusion (invasion) term incorporates the brain tissue heterogeneity, taking into account that high grade glioma invasion in WM is 5 times faster than in GM [31], by using locally different diffusion coefficients, $D(\mathbf{x})$. Moreover, in order to simulate the anisotropic invasion of glioma along white matter fibers, the local coefficients are multiplied by a matrix \mathbf{W} that describes the anisotropy of cell

diffusion along the 3-dimensional directions for each voxel. If the diagonal fiber directions are ignored, the local diffusion weighting tensor $\mathbf{W}(\mathbf{x})$ is a symmetric matrix of the following form:

$$\mathbf{W}(\mathbf{x}) = \begin{bmatrix} w_x(\mathbf{x}) & 0 & 0 \\ 0 & w_y(\mathbf{x}) & 0 \\ 0 & 0 & w_z(\mathbf{x}) \end{bmatrix} \quad (5)$$

$w_i(\mathbf{x}) \in [0,1]$, $i = x, y, z$ is the directional diffusion weight, which denotes the anisotropic diffusion of cell migration along the respective direction in position \mathbf{x} . \mathbf{W} denotes the contribution of each axis to the local direction of white fibers, while $D(\mathbf{x})$ actually denotes the scale of this parameter. Thus, by using these definitions, the local diffusion tensor \mathbf{D} in (3) is expressed as:

$$\mathbf{D}(\mathbf{x}) = D(\mathbf{x})\mathbf{W}(\mathbf{x}) \quad (6)$$

and the spatiotemporal diffusion reaction equation that describes glioma growth is equivalent to:

$$\frac{\partial c}{\partial t} = \text{div} \left((D(\mathbf{x})\mathbf{W}(\mathbf{x}))\nabla c \right) + f(c) \quad (7)$$

B. Using proportional local diffusion coefficients

In all proposed models, where tissue heterogeneity is simulated by using local diffusion coefficients, $D(\mathbf{x})$ takes two discrete values, that is D_g when voxel \mathbf{x} is located in GM and D_w when in WM. Usually, a fivefold difference between these two values is used, but this can also reach a 100-fold difference in very aggressive high grade glioma [31]. Thus, the brain is segmented into GM and WM, either by automatic segmentation or by mapping the real medical images on normal tissue atlases, for which a proportion of WM and GM cells is provided. In the latter case, real images are firstly registered to the atlas. Then, each image voxel is classified either as WM or as GM, according to the proportion of WM and GM in the respective

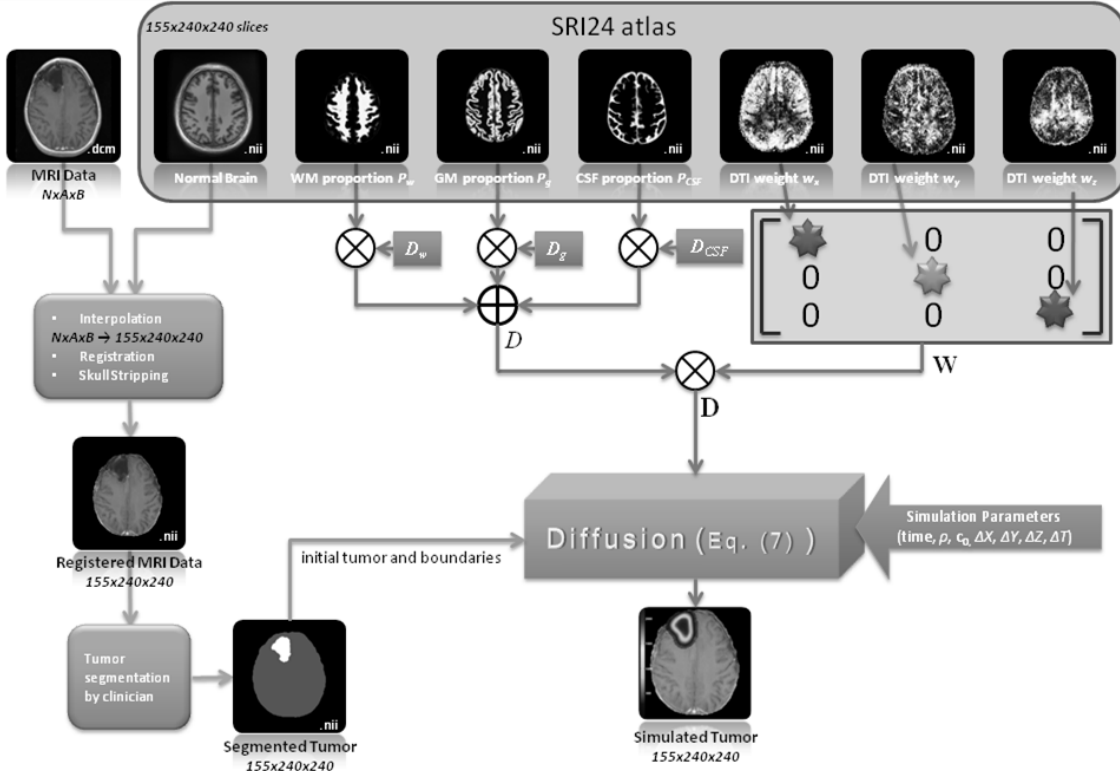


Fig. 1. Flow and overview of the proposed model.

atlas position. Consequently, if a voxel of the real data is mapped to a voxel in the atlas, for which the proportion of GM cells is 51% and the proportion of WM cells is 49%, then older approaches would classify this voxel as GM. However, this totally ignores the existence of WM and, hence, important information is truncated. Moreover, such models do not simulate glioma diffusion to CSF, although it has been observed that glioma cells may spread in the fluid.

What the current model suggests is to extend this idea and to fully utilize the continuous information on tissue matter, provided by atlases, such as the SRI24 normal brain atlas [45]. This atlas is generated by template-free non rigid registration from images of 24 normal brains. Except for the T1 and T2 MRI maps, the atlas provides the proportion $P_w(\mathbf{x})$ of WM, the proportion $P_g(\mathbf{x})$ of GM and the proportion $P_{CSF}(\mathbf{x})$ of CSF in each voxel \mathbf{x} . Thus, after registering medical data on the SRI24 atlas and setting the diffusion coefficient constants to D_g , D_w and D_{CSF} in WM, GM and CSF, respectively, the proportional local diffusion coefficient $D(\mathbf{x})$ can be calculated at each voxel \mathbf{x} as follows:

$$D(\mathbf{x}) = P_g(\mathbf{x})D_g + P_w(\mathbf{x})D_w + P_{CSF}(\mathbf{x})D_{CSF} \quad (8)$$

Hence, the model makes a total use of the proportion of white/gray matter in brain areas. Indeed, in the previous example, for which the proportion of GM and WM is 51% and 49% respectively, the voxel was classified as in GM, thus the respective diffusion coefficient is $D(\mathbf{x}) = D_g$. On the other hand, the proportional $D(\mathbf{x})$ for the same example is $D(\mathbf{x}) = 0.51D_g + 0.49D_w$, fully exploiting the atlas information of tissue proportion.

C. The local diffusion weighting tensor

In order to simulate the anisotropic growth of glioma along white matter tracts [46], the model uses the 3-by-3 local diffusion weighting tensor \mathbf{W} , which represents towards which direction the distribution of water diffusion extends the farthest. Moreover, SRI24 atlas provides the dominant eigenvectors of the diffusion tensor, which are produced as the covariance matrices of the 3D Gaussian probability distribution that models the water diffusion, at each voxel \mathbf{x} . These eigenvectors have been extracted from DTI. Thus, since $\mathbf{W}(\mathbf{x}) =$

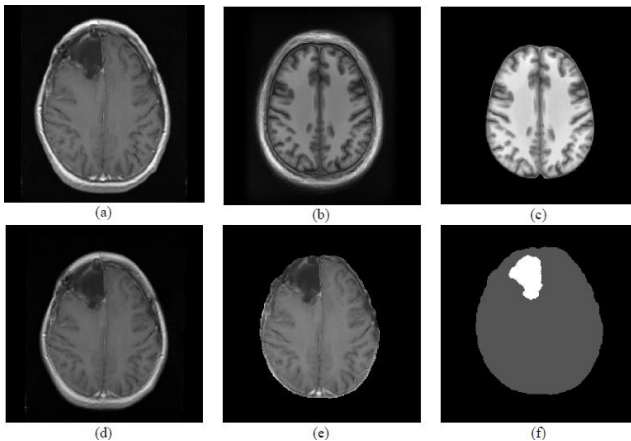


Fig. 2. (a) 8th slice of the initial 29-slice patient dataset before registration (b) the most similar to (a) unstripped slice of normal brain atlas (99th slice), (c) similar to (b) for stripped brain, (d) the 99th slice of the patient dataset after registration and interpolation, (e) the 99th image after skull stripping, (f) is annotated (d).

$\begin{bmatrix} w_x(\mathbf{x}) & 0 & 0 \\ 0 & w_y(\mathbf{x}) & 0 \\ 0 & 0 & w_z(\mathbf{x}) \end{bmatrix}$ is diagonal and $\begin{bmatrix} w_x(\mathbf{x}) \\ w_y(\mathbf{x}) \\ w_z(\mathbf{x}) \end{bmatrix}$ is an eigenvector of \mathbf{W} provided by SRI24, \mathbf{W} is directly provided by the eigenvectors of SRI24 atlas.

D. Data Acquisition

The model uses T1-MRIs taken from patients diagnosed with malignant glioblastoma multiforme. Such data for 9 patients has been provided by the Department for Pediatric Hematology and Oncology at the University Hospital of the Saarland, in Germany, for the needs of the ContraCancrum project [47], which aims at developing a composite multilevel platform for simulating malignant tumor development and response to therapeutic schedules. For all these datasets provided by Saarland University, there are two or more sessions taken on different dates, while therapy or surgery information has been provided, for tracking glioma development. However, because of its aggressive nature, the GBM is usually excised after diagnosis and for this reason only one case (without surgery or therapy) was found by the time this paper was written. However, 8 more cases were found were the partially excised tumor was followed up with imaging examinations while the patient received radiotherapy and simulations were performed in those specific intervals.

IV. SIMULATION

A. Data Preprocessing

The proposed model requires that both atlas and real data are registered and have the same form and size before applying modeling equations (7) and (8). In our test case, the patient dataset consists of 29 T1-MRI slices with unstripped skull (255×255 pixel images), while the SRI24 atlas provides 155 slices of normal brain (240×240 pixel images), with stripped and unstripped skull. Fig. 2 first slice (a) shows the 8th slice of the patient dataset, where the tumor has its largest size. The tumor is on the left frontal lobe. Images (b) and (c) depict the 99th slice of the SRI24 atlas normal brain, unstripped and stripped respectively. These are the most similar images to the real slice shown in (a).

Initially, the patient dataset has to be aligned to the midsagittal line, for correcting skew distortion before registering to the atlas using the MIPAV Application [http://mipav.cit.nih.gov/]. Next, the skull in the patient dataset is removed to match the stripped atlas images using fully-automated skull stripping technique, namely the Brain

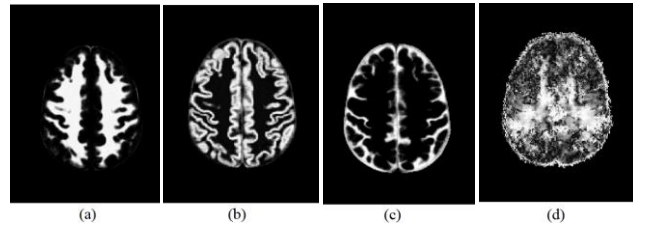


Fig. 3. The SRI24 atlas mappings for the proportion of (a) white matter (P_w), (b) gray matter (P_g) and (c) cerebrospinal fluid (P_{CSF}) and the one out of the three dominant eigenvector images (w_z), respective to the example of Fig. 2.

Extraction Tool (BET) [48].

The final registration step is done using the Optimized Automatic Registration 3D approach, by MIPAV. This method iteratively determines an optimal transformation of the image that globally minimizes a cost function (correlation ratio in our case), starting from the lowest resolution of the target image and moving to the highest (i.e. a simple blurring filter was applied to downgrade the resolution of the image). The optimum transformation is determined by the minimization of the correlation ratio (between target and reference images) computed for several rotation angles which vary from -30 to 30 degrees over the grid. The reference, as well as the target image are resampled and interpolated (using trilinear interpolation) to create high resolution isotropic voxels. Finally, the registration of the two images is completed by calculations performed to the center of mass from both images. The derived unstripped, registered and interpolated patient dataset consists of 155 slices with dimension 240×240 and being registered to the atlas. Fig. 2 (d) presents the 99th slice of the registered to the atlas patient dataset and (e) presents the same slice after skull stripping.

The last step, before handing data over simulation, is the delineation of the initial tumor boundaries provided by expert radiologists from the University of Saarland using the annotation and segmentation platform DoctorEye [http://biomodeling.ics.forth.gr]. This is shown in Fig. 2 (f) (in white). Summarizing, after acquiring the stripped, registered, interpolated and annotated dataset, diffusion simulation can be performed.

Patient image data can now be directly mapped to the SRI24 atlas, where $D(\mathbf{x})$ and $\mathbf{W}(\mathbf{x})$ for solving Equation (7) are available. Following the current example, Fig. 3 (a-d) presents the respective mappings of the P_w , P_g , P_{CSF} and one of the three coordinates of the dominant eigenvector (w_2). It is important to mention that because these coefficients depict proportions of brain matter and directionality measures, the image values are ranged in $[0,1]$. On the other hand MRIs in Fig. 2 (a-d) take discrete intensity values in $[0, 1, \dots, 255]$.

B. Solver

Equation (7) is a second order partial differential equation that can be solved using numerical methods, such as Finite Differences, Finite Elements, Monte Carlo, spectral and variational methods [49]. Due to storage limitations and in order the glioma model to be computationally consistent, as analyzed in [50], we have used the mathematical framework of Finite Differences proposed in [51] with Verhulst (logistic) proliferation. More specifically, the implicit scheme of Crank Nikolson Finite Differences has been implemented to solve equation (7) in three dimensions. Parameters for the simulation have been chosen according to bibliography, for high grade glioma [52], as stated in the next section.

C. Experimental Data and Choice of Parameters

As already explained, one real temporal glioma case was chosen on the basis that no surgery was performed and no therapy given to the patient (Fig. 2) for demonstrating our method in detail, consisting of two sets of 29 T1-MRI slices, taken from two different post-treatment sessions. The respective T2 MRIs were also available and were used for estimating how well the model parameters D and ρ , extracted

from bibliography [52], approached the values derived with the method proposed by Harpold et al. [37, 53].

This specific patient suffered from inoperable glioblastoma and did receive irradiation for 2 months, till 17-12-2009, concurrently with temolozolomide treatment. Then, the tumor was stable for 16 days and progressed again. The first dataset of MRI slices after treatment was acquired on 31-3-2010, while the second set on 31-5-2010. Thus, the tumor progression within that 60-day post-treatment period can be approximated as a free-growth procedure, i.e. $T(t)=0$. Similarly, the rest 8 datasets were intentionally picked from similar cases (with post-operation relapse of tumor), so as to model glioma growth as free- growth procedure for the respective period of time for each case.

The proliferation parameter ρ was set to the constant value of $\rho=0.012 \text{ day}^{-1}$ corresponding to the observed rate of high-glioma [52], as provided in bibliography. Similarly, the constant values D_w and D_g for diffusion were picked from bibliography as $0.010 \text{ mm}^2/\text{day}$ and $0.002 \text{ mm}^2/\text{day}$ respectively. These values were found to meet the values derived with the method proposed by Harpold et al. [37, 53], for estimating the ratio D/ρ by using the two T1 and T2 MRI sessions. For the rest 8 cases, ρ was set to the constant value 0.012 day^{-1} . On the other hand, D_w and D_g were picked from [52], for high glioma values, to optimally correspond to the respective values of D , estimated by Harpold's method for $\rho=0.012 \text{ day}^{-1}$.

Continuing, because the CSF is rarely invaded by glioma cells, a first approach adopted for simulating diffusion in CSF was to set a very small diffusive coefficient as $D_{CSF}=0.01 D_w$. The value of D_{CSF} was not arbitrarily chosen, but it has been estimated by applying the method of Harpold et al. on a different provided dataset where CSF has been infected by glioma cells. Thus, the ratio D_{CSF}/ρ was estimated in the CSF area, by using two T1 and T2 MRI sessions.

Moreover, the initial concentration for the tumor voxels was set at $200 \text{ cells}/\text{mm}^3$ and the Verhulst law parameter for the maximum concentration was defined as $c_m=10^6 \text{ cells}/\text{mm}^3$. Lastly, the simulation grid dimensions were defined as $\Delta X = \Delta Y = \Delta Z = 1 \text{ mm}$, the time step was defined as $\Delta T = 1 \text{ h}(1/24 \text{ day})$ and the overall modeling time of cell progression was 60 days, as in the real clinical case.

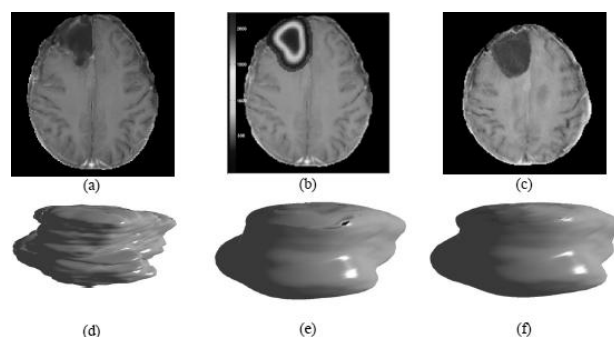


Fig. 4. Some simulation results; Up: the 99th slice of the (a) initial tumor, (b) the simulated final tumor, mapped on (a), and the (c) real final tumor. Down: the 3-dimensional reconstructions of (d) the initial annotated tumor, (e) the simulated tumor after 60 days and (f) the real annotated tumor after 60 days.

D. Simulation Results

After extracting the required datasets using the SRI24 atlas and after defining the simulation parameters, the proposed model of equation (7) can be applied on the real annotated clinical case. Fig. 4 (a) presents the 99th slice of the initial tumor, as produced after data preprocessing and (b) shows the respective simulated glioma concentration after 60 days of progression, mapped on the initial dataset. On the other hand, Fig. 4 (c) presents the respective real final tumor, as provided by the clinicians. Lastly, Fig. 4 (d) depicts the 3-dimensional perspective of the initial brain tumor. Fig. 4 (e) presents the simulated tumor after 60 days, while (f) presents the real tumor, derived after registering and interpolating the real tumor (second session) to the atlas. The visualization threshold of the simulated tumor concentration was set to 400 cells/mm³ [52].

In order to better evaluate the efficiency and the practical usefulness of the model, it is important to conduct a large number of simulations with real data, especially datasets with the characteristic fingering invasion of glioma. However, from the figures reported here, there seems to be a good qualitative agreement between the real and the simulated tumor growth. The next step is to evaluate the performance of the proposed model using all nine datasets, comparing it to the two standard diffusive models: uniform radial growth across all tissue types and faster diffusion in white matter with discrete diffusion coefficients.

E. Evaluation

We have made simulations on a series of nine datasets in order to compare the simulated tumor with the final actual tumor, as annotated by the radiologists. In the eight other cases however, the tumor was treated with radiotherapy which isn't currently taken into consideration in the models compared. For evaluation, we used a scheme that uses solid metrics and provides objective comparison. Therefore, the annotated final tumor serves as a golden ground truth and the Jaccard (JC), Dice (DS) and Volume Similarity (VS) metrics are adopted [54]. These metrics are defined as:

$$\begin{aligned} JC &= TP / (FP + TP + FN) \\ DS &= 2TP / (FP + 2TP + FN) \\ VS &= 1 - |FP - FN| / (FP + 2TP + FN) \end{aligned} \quad (9)$$

where TP (True Positive) is the number of tumor voxels belonging to both ground truth and simulated result, FP (False Positive) is the number of tumor voxels belonging to simulated result and not belonging to ground truth and FN (False Negative) is the number of tumor voxels belonging to ground truth but not belonging to simulated tumor.

The evaluation metrics have been calculated on the

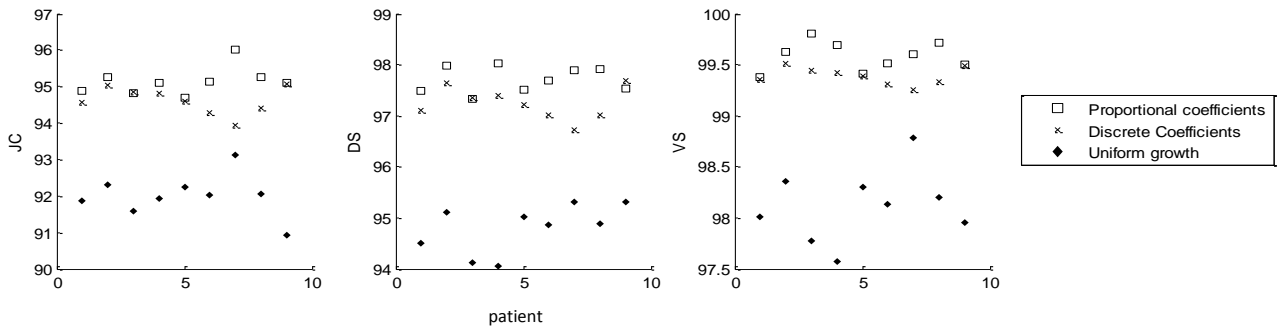


Fig. 5 – Scatter plot of JC, DS and VS (%) for 9 cases where the proportional, the discrete and the uniform growth models have been applied.

simulation results of the nine patient datasets. On each dataset, three different models have been applied; the proportional model, the model with uniform tumor growth and the model with discrete values for $D(\mathbf{x})$. After running all three models for each dataset, the metrics for each one have been calculated. Finally, the average metrics for each model have been estimated.

The scatter plots of the three metrics are presented in Fig. 5. For the proportional model, the average JC is 0.54% higher than the discrete model and 3.39% higher than the uniform growth model. Similarly, the average DS for the proportional model is 0.48% and 3.07% higher than the discrete and the uniform model, respectively. Lastly, the average VS is 0.19% and 1.49% higher for the proposed model, compared to the results of the discrete and the uniform growth model, respectively. Thus, the results indicate that there is a potential advantage of the probabilistic diffusion coefficients over uniform and discrete diffusion parameters.

V. DISCUSSION

Computational modeling of glioma growth by using the proliferation – diffusion equation was initiated before 15 years and has developed fast. Several variations of the equation have been proposed up to now, so as to include different biological patterns, such as faster tumor diffusion in white matter or facilitated migration along white matter fibers. The current proposed model adopts the results of the most prominent models [21, 22, 24] and extends their functionality. The first applications on real patient datasets, of the continuous proportional diffusion coefficients, proposed in this paper, instead of the discrete two-value coefficients, seem to slightly improve the average performance of these models. This indicates that using proportions of tissue matter on each voxel, instead of classifying them either in GM or WM, valuable information is not truncated and the model simulates more accurately the actual tumor growth.

The proportional model requires the a priori knowledge of WM, GM and CSF matter proportions and the directions of the WM tracts in brain. Therefore, structural and statistical information of brain is extracted by open-access brain atlases, such as SRI24. By mapping clinical MRI data to a brain matter atlas, it is possible to approximate the required tissue information / composition in the tumor area, since this is not possible to extract from the real MRI data we had access in this work. Hence, simulation using local diffusion coefficients on real MRI images becomes possible, even if the lesion “hides” the underlying tissue. This of course, is an approximation and

the added value can only be assessed through extending the gold truth experiments / results presented herein. However, it should be stressed that GBM follow ups without surgery are rare since surgery is performed in almost all cases after diagnosis rendering impossible to assess actual temporal tumor evolution. For this reason we work closely with our clinical partners to maximize the number of cases where the models can be validated against the actual tumor change.

Apart from the commonly used GM and WM tissue information, CSF proportion is also provided and utilized for simulating the rare cases of glioma, in which the cerebrospinal fluid has been invaded by tumor cells [42]. Tumor expansion in CSF has been modeled by applying a non-zero diffusion coefficient. In the current experiments, the initial tumor size was not so large to allow tumor cells migrate into CSF, as in real cases. However, in experiments for large glioblastoma, where CSF might get infected, tumor cells have appeared in the CSF areas. Chemotherapy and radiotherapy can also be simulated with the current model (this is part of our ongoing work), after adjusting the treatment term $T(t)$, which has been described in the therapy section accordingly. The term is entailed in the proportional model and the only remaining issue is to estimate the optimal therapy parameters. Therefore, several techniques have been proposed towards simulating therapy treatment and surgery. These have been adjusted to diffusive models and cover the cases of resection [36], radiotherapy [37, 38] and chemotherapy [23, 52]. Consequently, such a method for modeling therapy could also be combined with the framework presented in this paper.

VI. CONCLUSION

This paper presents an extended methodology for modeling GBM and predicting the progress of glioblastoma multiforme in space and in time. The diffusion – reaction equation was used for simulating the spatiotemporal change of tumor cell concentration, taking into consideration partial gray and white matter concentration in each voxel. Diffusion coefficients for WM, GM and CSF were extracted from the SRI24 open brain atlas. Moreover, the atlas DTI - MRIs were used for calculating the directional local diffusion tensors, representing the directions of white matter tracts.

The results of simulating free tumor growth indicate that there might be a potential advantage of the probabilistic diffusion coefficients over fixed-discrete diffusion parameters. This is an important finding that needs to be further validated both from the experimental and the biological interpretation sides. Moreover, the reported cases in this paper do not show mass effect, nor the characteristic diffusive fingers of glioma, which should be further studied with larger and more aggressive gliomas. For this reason we are currently working on a large number of glioma cases that have been provided for the purposes of the ContraCancrum project.

The first approach of setting a non-zero diffusion coefficient to CSF, which has been followed here, has not yet been studied in depth for real cases where CSF invasion has been diagnosed by radiologists. For these cases it would be interesting to study if fluid dynamics could better approximate the migration of cells in CSF and simulate solid/fluid structure interaction.

Predicting the tumor shape and volume, especially dependant on therapy parameters, could become a powerful tool for the clinicians, who could then adjust their therapy schemes also according to the parameters that yield the optimal prediction outcome for the specific patient. This will have an enormous impact in improving individualized therapy planning and promoting patient's quality of life by minimizing side effects, due to inadequate treatment.

REFERENCES

- [1] WHO, "http://www.who.int/mediacentre/factsheets/fs297," World Health Organization. Retrieved 2010-11-15.
- [2] P. Boyle, and B. Levin, "World Cancer Report 2008," IARC, 2010.
- [3] Brain Tumors, "http://www.abta.org", American Brain Tumor Association. Retrieved 2010-11-15.
- [4] Central Brain Tumor Registry of the United States, "Statistical Report: Primary Brain Tumors in the United States, 1992-1997.", Chicago, 2000.
- [5] M. Tovi, "MR Imaging in cerebral gliomas analysis of tumour tissue components," *Acta Radiol Suppl*, Vol. 384, pp: 1-24, 1993.
- [6] S. Price, N. Burnet, T. Donovan, H. Green, A. P. Na, N. Antoun, J. Pickard, T. Carpenter, and J. Gillard, "Diffusion tensor imaging of brain tumours at 3t; A potential tool for assessing white matter tract invasion?," *Clin Radiol*, vol. 58, pp. 455-462, 2003.
- [7] P. Lissoni, S. Meregalli, L. Nosetto, S. Barni, G. Tancini, V. Fossati, and G. Maestroni, "Increased survival time in brain glioblastomas by a radionuclide endocrine strategy with radiotherapy plus melatonin compared to radiotherapy alone," *Oncol*, vol. 53, no. 1., pp. 43-6, 1996.
- [8] E. Van Meir, C. Hadjipanayis, A. Norden, H. K. Shu, P. Y. Wen, and J. Olson, "Exciting New Advances in Neuro-Oncology: The Avenue to a Cure for Malignant Glioma," *CA: Cancer Jfor Clin*, vol. 60, no. 3, pp. 166-93, 2010.
- [9] D. Krex, B. Klink, C. Hartmann, A. Von Deimling, T. Pietsch, M. Simon, M. Sabel, J. P. Steinbach, et al., "Long-term survival with glioblastomamultiforme," *Brain*, vol. 130, no. 10, pp. 2596-606, 2007.
- [10] University of California, Los Angeles Neuro-Oncology: How Our Patients Perform: GlioblastomaMultiforme [GBM]. neurooncology.ucla.edu. Retrieved on 2010-11-19.
- [11] K. Swanson, E. Alvord, and J. Murray, "Virtual brain tumours (gliomas) enhance the reality of medical imaging and highlight inadequacies of current therapy," *BrJCancer*, vol. 86, pp. 14-18, 2002.
- [12] D. Silbergeld, R. Rostomily, and Jr. Alvord, "The cause of death in patients with glioblastoma is multifactorial: Clinical factors and autopsy findings in 117 cases of supratentorial glioblastoma in adults," *J NeuroOncol*, vol. 10, pp. 179 – 185, 1991.
- [13] A. Claes, A. Idema, and P. Wesseling, "Diffuse glioma growth: a guerilla war," *Acta Neuropathol*, vol. 114, no. 5, pp. 443-458, 2007.
- [14] S. Toms, W. Lin, R. Weil, M. Johnson, E. Jansen, and A. Mahadevan-Jansen, "Intraoperative optical spectroscopy identifies infiltrating glioma margins with high sensitivity," *Neurosurg*, vol. 57, no. 4, pp. 382-91, 2005.
- [15] H. Frieboes, X. Zheng, C. H. Sun, B. Tromberg, R. Gatenby, and V. Cristini, "An Integrated Computational/Experimental Model of Tumor Invasion," *Cancer Res*, vol. 66, pp. 1597, 2006.
- [16] S. Sjöström, U. Andersson, Y. Liu, T. Brännström, H. Broholm, C. Johansen, H. Collatz-Laier, R. Henriksson, M. Bondy, and B. Melin, "Genetic variations in EGF and EGFR and glioblastoma outcome," *NeuroOncol*, vol. 12, no.8, pp. 815-821, 2010.
- [17] V. Cristini, J. Lowengrub, Q. Nie, "Nonlinear simulation of tumor growth," *JMathBiol*, vol. 46, pp. 191-224, 2003.
- [18] T. Deisboeck, M. Berens, A. Kansal, S. Torquato, A. Stemmer-Rachamimov, and E. Chiocca, "Pattern of self-organization in tumour systems: complex growth dynamics in a novel brain tumour spheroid model," *Cell Prolif*, vol. 34, no. 2, pp. 115-34, 2001.
- [19] D. Drasdo, and S. Höhme, "A single-cell-based model of tumor growth in vitro: monolayers and spheroids," *PhysBiol*, vol. 2, pp. 133-147, 2005.
- [20] P. Tracqui, "From passive diffusion to active cellular migration in mathematical models of tumor invasion," *Acta Biblioth*, vol. 43, pp. 443-464, 1995.
- [21] K. Swanson, E. Alvord, and J. Murray, "A Quantitative Model for Differential Motility of Gliomas in Grey and White Matter," *Cell Prolif*, vol. 33, no. 5, pp. 317-330, 2000.

- [22] S. Jbabdi, E. Mandonnet, and H. Duffau, "Simulation of anisotropic growth of low-grade gliomas using diffusion tensor imaging," *MagnReson Med*, vol. 54, pp. 616-24, 2005.
- [23] G. Stamatakos, E. Kolokotroni, D. Dionysiou, E. Georgiadi, and C. Desmedt, "An advanced discrete state - discrete event multiscale simulation model of the response of a solid tumor to chemotherapy: Mimicking a clinical study," *JTheorBiol*, vol. 266, pp. 124-139, 2010.
- [24] O. Clatz, M. Sermesant, P. Bondiau, H. Delingette, S. K. Warfield, G. Malandain, and N. Ayache, "Realistic simulation of the 3-D growth of brain tumours in MR images coupling diffusion with biomechanical deformation," *IEEE Trans on Med Im*, vol. 24, pp. 1334-1346, 2005.
- [25] E. Konukoglu, O. Clatz, B. Menze, M. A. Weber, B. Stieltjes, E. Mandonnet, H. Delingette, and N. Ayache, "Image Guided Personalization of Reaction Diffusion Type Tumor Growth Models using Modified Anisotropic Eikonal Equations," *IEEE Transon MedIm*, vol. 29, no. 1, pp. 77-95, 2010.
- [26] C. Hogue, C. Davatzikos, and G. Biros, "Modeling glioma growth and mass effect in 3D MR images of the brain," *ProcMICCAI*, vol. 4791, pp. 642-650, 2007.
- [27] A. Roniotis, K. Marias, V. Sakkalis, and M. Zervakis, "Diffusive modelling of glioma evolution: a review," *Jof BiomSciEng, ScientRes*, vol. 3, no. 5, pp.501-508,2010.
- [28] A. Kansal, S. Torquato, G. Harsh, et al., "Simulated brain tumor growth dynamics using a three-dimensional cellular automaton," *J TheorBiol*, vol. 203, pp. 367-382, 2000.
- [29] A. Zizzari, "Methods on Tumor Recognition and Planning Target Prediction for the Radiotherapy of Cancer," PhD Thesis, Electronics Dept, University of Magdeburg, 2004.
- [30] M. Tabatabai, D. Williams, and Z. Bursac, "Hyperbolic growth models: theory and application," *TheorBiolMedModel*, vol. 2, no. 1, pp. 14, 2005.
- [31] A. Giese, and M. Westphal, "Glioma Invasion in the Central Nervous System," *Neurosurg*, vol. 39, no. 2, pp. 235-252, 1996.
- [32] A. Giese, R. Bjerkvig, M. Berens, and M. Westphal, "Cost of Migration: Invasion of Malignant Gliomas and Implications for Treatment," *J ClinOncol*, vol. 21, no. 8, pp. 1624 - 1636, 2003.
- [33] T. Conturo, N. Lori, T. Cull, E. Akbudal, A. Snyder, J. Shimony, R. McKinstry, H. Burton, and M. Raichle, "Tracking neuronal pathways in the living human brain," *ProcNatAcadSci*, vol. 96, pp. 10422-10427, 1999.
- [34] M. Morris, R. Greiner, J. Sander, A. Murtha, and M. Schmidt, "A Classification-Based Glioma Diffusion Model Using MRI Data," *AdvArtifIntell, LectNotin CompSci*, vol. 4013, pp. 98-109, 2006.
- [35] M. Marusic, Z. Bajzer, J. P. Freyer, S. Vuk-Palovic, "Analysis of growth of multicellular tumour spheroids by mathematical models," *Cell Prolif*, vol. 27, pp. 73-94, 1994.
- [36] K. Swanson, R. Rostomily, E. Alvord, "A mathematical modeling tool for predicting survival of individual patients following resection of glioblastoma: A proof of principle," *Br J Cancer*, vol. 98, pp. 113-119, 2008.
- [37] R. Rockne, J. K. Rockhill, M. Mrugala, A. M. Spence, I. Kalet, K. Hendrickson, A. Lai, T. Cloughesy, E. C. Alvord, and K. Swanson, "Predicting the efficacy of radiotherapy in individual glioblastoma patients in vivo: a mathematical modeling approach," *Phy MedBiol*, vol. 55, pp. 3271-3285, 2010.
- [38] E. Hall, "Radiobiology for the Radiologist," *J B Lippincott*, Philadelphia, 1994.
- [39] G. Stamatakos, V. Antipas, N. Uzunoglu, and R. Dale, "A four-dimensional computer simulation model of the in vivo response to radiotherapy of glioblastomamultiforme: studies on the effect of clonogenic cell density," *Br J Radiol*, vol. 79, pp. 389-400, 2006.
- [40] G. Stamatakos, V. Antipas, N. Ozunoglu, "A patient-specific in vivo tumor and normal tissue model for prediction of the response to radiotherapy," *Math Inf Med*, vol. 46, pp. 367-375, 2007.
- [41] V. Sakkalis, A. Roniotis, C. Farmaki, I. Karatzanis, and K. Marias, "Evaluation framework for the multilevel macroscopic models of solid tumor growth in the glioma case," *ConfProc IEEE Eng Med BiolSoc*, vol. 1, pp. 6809-6812, 2010.
- [42] K. Onda, K. Tanaka, R. Takahashi, H. Takeda, N. Ikuta, F., "Symptomatic cerebrospinal fluid dissemination of cerebral glioblastoma. Computed tomographic findings in 11 cases," *Neuroradiol*, vol. 32, no. 2, pp. 146-50, 1990.
- [43] G. Dohrmann, J. Farwell, and J. Flannery, "Glioblastomamultiforme in children," *J Neurosurg*, vol. 44, pp. 442-448, 1976.
- [44] T. Rohlfing, N. Zahr, E. Sullivan, and A. Pfefferbaum, "The SRI24 multichannel atlas of normal adult human brain structure," *HumBrMap*, vol. 31, no. 5, pp. 798-819, 2010.
- [45] <http://nitrc.org/projects/sri24>
- [46] K. Saladin, "Anatomy & Physiology. The Unit of Form and Function, Edition 5," pp. 451-490, McGraw-Hill, NY, 2007.
- [47] K. Marias, D. Dionysiou, V. Sakkalis, N. Graf, R. M. Bohle, P. V. Coveney, S. Wan, A. Folarin, P. Büchler, M. Reyes, G. Clapworthy, E. Liu, J. Sabczynski, T. Bily, A. Roniotis, M. Tsiknakis, E. Kolokotroni, S. Giatili, C. Veith, E. Messe, H. Stenzhorn, Y. J. Kim, S. Zasada, A. N. Haidar, C. May, S. Bauer, T. Wang, Y. Zhao, M. Karasek, R. Grewer, A. Franz, and G. Stamatakos, "Clinically driven design of multi-scale cancer models: the ContraCancrum project paradigm," *J R SocInterf Focus*, Published online March 30, 2011, doi: 10.1098/rsfs.2010.0037.
- [48] S. Smith, "Fast robust automated brain extraction," *HumBrainMappvol*, 17, pp. 143-155, 2002.
- [49] D. Gottlieb, and A. Orszag, "Numerical Analysis of Spectral Methods: Theory and Applications," *S.I.A.M.*, Philadelphia, 1977.
- [50] A. Roniotis, K. Marias, V. Sakkalis, G. Stamatakos, and M. Zervakis, "Comparing Finite Element and Finite Difference Techniques As Applied to the Development of Diffusive Models of GlioblastomaMultiforme Growth," *IEEE Engin Medand BiolSocConf*, 2010.
- [51] A. Roniotis, K. Marias, V. Sakkalis, G. Tsibidis, and M. Zervakis, "A Complete Mathematical Study of a 3D Model of Heterogeneous and Anisotropic Glioma Evolution," *IEEE Eng in Med and BiolSocConf*, vol. 1, pp. 2807-2810, 2009.
- [52] G. Powathil, M. Kohandel, A. Oza, and M. Milosevic, "Mathematical modeling of brain tumours: effects of radiotherapy and chemotherapy," *Phys MedBiol*, vol. 52, pp. 3291-3306, 2007.
- [53] H. Harpold, E. Alvord, and K. Swanson, "The evolution of mathematical modeling of glioma proliferation and invasion," *J NeuropExpNeurol*, vol. 66, pp. 1-9, 2007.
- [54] J. Udupa, V. LaBlanc, H. Schmidt, C. Imielinska, P. Saha, G. Grevera, Y. Zhuge, P. Molholt, Y. Jind, and L. Currie, "A methodology for evaluating image segmentation algorithms," *SPIE MedIm2002: ImProc*, pp. 266-77, 2002.



Alexandros Roniotis is a Ph.D. candidate in the Dept of Electronics and Computer Engineering in the Technical University of Crete. In 2006 he graduated with distinction from the Dept of Informatics and Telecommunications, University of Athens and took his M.Sc. in Signal Processing and Communications, Electrical & Electronic Engineering Dept of Imperial College London in 2007. Since 2008 he works in the Institute of Computer Science - Foundation for Research and Technology (ICS - FORTH). His research interests include modeling of biological processes; biomedical imaging, digital image processing and pattern recognition.



Georgios C. Manikis holds a Master degree in Electronics and Computer Engineering from the Technical University of Crete. He now works in the Laboratory of Computational Medicine, in the Institute of Computer Science - Foundation for Research and Technology (ICS - FORTH). His research interests include image processing, biostatistics and pattern recognition with applications in classification, feature extraction and data integration.



Vangelis Sakkalis holds a Ph.D. in Electronics and Computer Engineering from the Technical University of Crete. Previously he completed his Masters degree at Imperial College of Science, Technology and Medicine, UK. He holds an Associate Researcher position in the Institute of Computer Science - Foundation for Research and Technology (ICS - FORTH). His background falls in Computational Medicine, Biomedical Engineering, Atomic-Molecular Physics, Optoelectronics and Laser. His research interests include biosignal and image analysis, visualization, classification algorithms, biostatistics and biomedical informatics and modeling.



Michalis E. Zervakis holds a Ph.D degree from the University of Toronto, Department of Electrical Engineering, since 1990. He joined the Technical University of Crete on January 1995, where he is serving as Professor at the department of Electronic and Computer Engineering. He served as Associate Editor in the "IEEE Transactions on Signal Processing" from 1994 to 1996. He was an assistant professor with the University of Minnesota-Duluth, USA, from September 1990 to December 1994. Prof.

Zervakis is the director of the Digital Image and Signal Processing Laboratory (DISPLAY) at the Technical University of Crete. Under his direction, the lab is involved in research on modern aspects of signal processing, including estimation and constrained optimization, multi-channel and multi-band signal processing, wavelet analysis for data/ image processing and compression, neural networks and fuzzy logic with applications in biomedical data analysis, imaging systems and integrated automation systems. Developments also include DSP-based real-time implementation.



Ioannis Karatzanis holds a BSc in Physics from the University of Crete. He is a member of the technical team of the Computational Medicine Laboratory in the Institute of Computer Science of the Foundation for Research and Technology – Hellas (CML - ICS - FORTH), where he is involved in the development of user interfaces for medical applications (both for clinical environment and for home environment), Digital Image Processing, Signal Processing and Analysis, and many more...



Dr. Kostas Marias holds a Principal Researcher position in the Institute of Computer Science (ICS - FORTH), leading the Computational Medicine Laboratory (CML). During 2001 - 2003, he worked as a Researcher at the University of Oxford after completing his PhD in the field of Medical Image Analysis. He also holds an MSc degree from Imperial College of Science, Technology and Medicine in Physical Science and Engineering in Medicine as well as an Electrical Engineering Diploma from the

National Technical University of Athens (N.T.U.A). His current research interests are in the areas of medical image analysis, registration and fusion and cancer modeling.